

Heterogeneous catalytic performance and stability of iron-loaded ZSM-5, Zeolite-A, and

Silica for phenol degradation: A microscopic and spectroscopic approach

Yasaman Ghaffari^{a,b}, Nishesh Kumar Gupta^{a,b}, Suho Kim^{a,b}, Kwang Soo Kim^{a,b*}

a. University of Science and Technology, Republic of Korea

b. Department of Land, Water, and Environment Research, Korea Institute of Civil Engineering and Building Technology, Republic of Korea

Section 1. Synthesis of catalysts

Crystalline Fe-Zeolite A: Fe-Zeolite-A was synthesized in a hydrothermal reactor by the Sol-Gel method. Sodium silicate (Na_2SiO_3) and sodium aluminate (NaAlO_2) were used as silica and alumina source, respectively. 17.19 g of Na_2SiO_3 and 13.33 g of NaAlO_2 were dissolved separately in 225 ml of distilled water. 2.25 g of AIC was used as an iron source and dissolved in 60 ml distilled water. The iron solution and NaAlO_2 solution were poured to Na_2SiO_3 solution with continuous stirring to make a gel mixture. The mixture gel was placed on a shaking incubator for 24 h at 25 °C for aging. The aged mixture was then transferred to a hydrothermal reactor and kept at 120 °C for 48 h. Then, the synthesized product was rinsed with distilled water until the filtrate pH reached 8.0. Sample was dried at 100 °C in a drying oven overnight. Finally, the dried sample was transferred for calcination at 500 °C for 5 h to eliminate organic compounds like citrate. The molar ratio of Na_2O : SiO_2 : Al_2O_3 : Fe: H_2O mixture was chosen as 3.1: 2.0: 1.0: 0.1: 400.9. The sample was coded as Fe-Zeo-A.

Crystalline Fe-ZSM-5: Fe-ZSM-5 was prepared from 40% SiO_2 , NaOH, NaAlO_2 , and TPAOH (as a structure-directing agent) via the hydrothermal method. Exactly 3.74 g of NaAlO_2 and 7.98 g of NaOH were dissolved separately in 120 ml of distilled water. 10 g of AIC was dissolved in

85 ml of distilled water. Then, 150 ml of silica sol was transferred to a beaker, and 30 ml of TPAOH was added dropwise into the silica sol with continuous stirring. Then NaAlO₂, NaOH and AIC solutions were added dropwise to the TPAOH and silica sol mixture.

The gel solution was transferred to an incubator for aging at 50 °C and stirring at 200 rpm for 24 h. The mixture was then transferred to a steel autoclave lined with Teflon for the hydrothermal reaction at 180 °C for 48 h. Then, the synthesized product was rinsed with distilled water until the filtrate pH reached 8.0. The material was dried at 100 °C for 5 h. Finally, the dried material was calcined at 550 °C for 6 h. The synthesis mixture comprises of the following molar ratio 6.2 Na₂O: 50.4 SiO₂: 1.0 Al₂O₃: 1.5 TPAOH: 1.0 Fe₂O₃: 1248.3 H₂O. The sample was coded as Fe-ZSM-5.

Amorphous Fe-containing silica (Fe₂O₃-Silica): Sol-Gel method was used for synthesizing this catalyst. First, 0.15 g of iron acetate was dissolved in 60 ml of CTAC solution, and then 60 ml of TEOS was added to the mixture. After that, the mixture was transferred to an incubator for aging at 25 °C and stirring at 200 rpm for 24 h. The solid material was calcined at 550 °C for 6 h. The synthesis mixture comprises of the following molar ratio 1.0 TEOS: 0.7 CTAC: 0.003 iron acetate. The sample was coded as Fe-Silica.

Section 2. Characterization of catalysts

Supplementary Table 1. Elemental analysis of Fe-ZSM-5, Fe-Zeo-A, and Fe-Silica

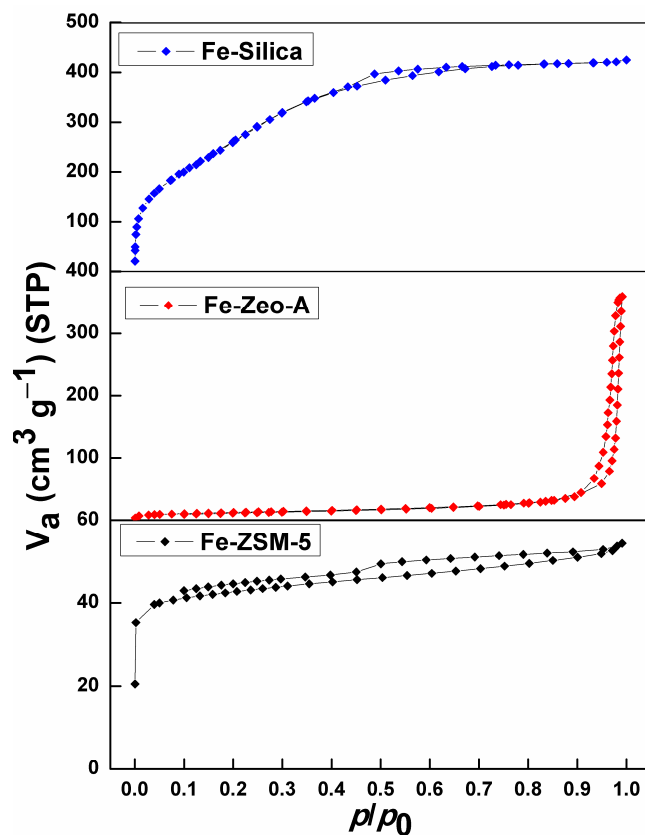
Element	Fe-ZSM-5	Fe-Zeo-A	Fe-Silica
	Weight%	Weight%	Weight%
O	62.23	60.98	80.54
Na	0.46	4.41	-

Al	2.92	14.36	-
Si	33.06	19.23	19.04
Fe	1.33	1.02	0.42

BET: Porosity properties and specific surface areas of Fe-based zeolites and silica were analyzed by N₂ adsorption-desorption isotherms (**Supplementary Figure 1**). The N₂ isotherm of Fe-ZSM-5 showed a hysteresis loop at a high relative pressure fit for Type IV of adsorption isotherm, which is the characteristic of mesoporous materials. Whereas, for Fe-Zeo-A, Type III isotherm was the most suitable one and is marked as a nonporous or macroporous solid. For Fe-Silica, Type I(b) isotherm was suitable for describing N₂ adsorption-desorption isotherm and is an indication of a broad range of microporosity [1]. The specific surface areas (S_{BET}), micropore volume (V_{micro}), and mesopore volume (V_{meso}) estimated using the Brunauer-Emmett-Teller method, t-plot, and Barrett-Joyner-Halenda method, respectively along with the total pore volume (V_{t}) and average pore diameter ($D_{\text{p,avg}}$) have been tabulated in **Supplementary Table 2**.

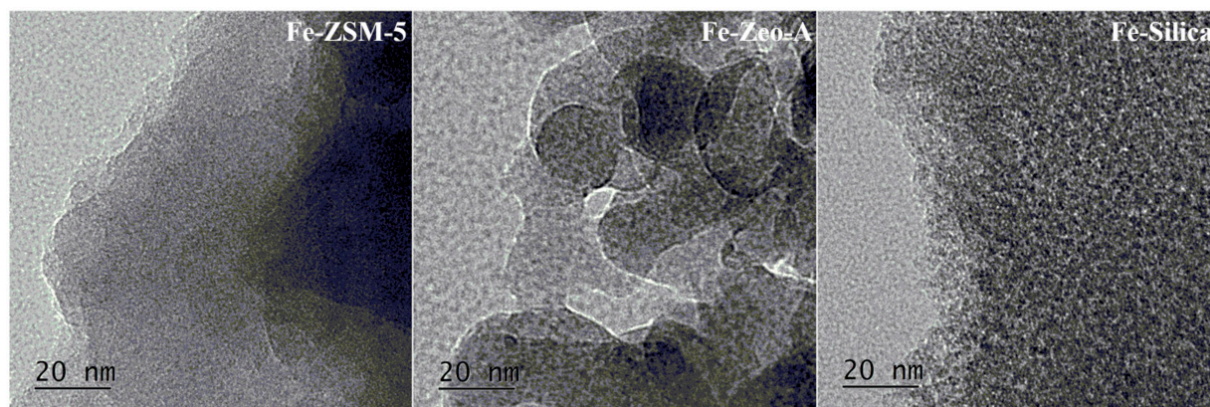
Supplementary Table 2. Physicochemical properties of Fe-ZSM-5, Fe-Zeo-A, and Fe-Silica.

Sample	S_{BET} ($\text{m}^2 \text{g}^{-1}$)	V_{t} ($\text{cm}^3 \text{g}^{-1}$)	V_{micro} ($\text{cm}^3 \text{g}^{-1}$)	V_{meso} ($\text{cm}^3 \text{g}^{-1}$)	$D_{\text{p,avg}}$ (nm)
Fe- ZSM-5	326.21	0.169	0.1181	0.0536	2.0713
Fe-Zeo-A	45.45	0.536	-	0.5316	47.1370
Fe-Silica	1088.50	0.654	0.6056	0.5139	2.4032



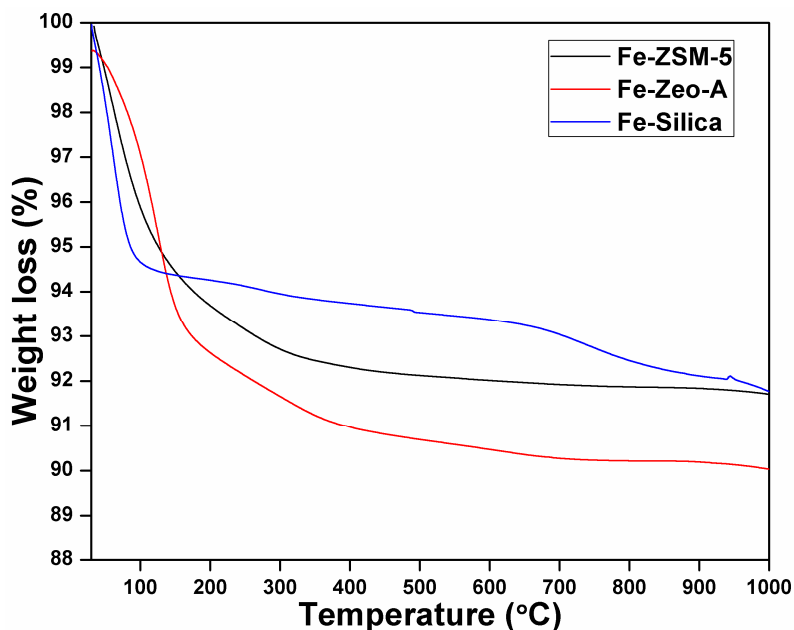
Supplementary Figure 1. N_2 adsorption-desorption isotherms of catalysts at 77 K.

TEM: The TEM image of Fe-ZSM-5 showed no Fe_2O_3 aggregates indicating that Fe was partly incorporated in the framework (Fe in place of Al) and majorly was in a highly dispersed state in the zeolitic structure as oxide (**Supplementary Figure 2**). However, for Fe-Zeo-A and Fe-Silica, iron oxide was found distributed non-uniformly in the catalysts (**Supplementary Figure 2**). EDX analysis showed that the iron content in Fe-ZSM-5 (1.33 wt.%) was higher than that of Fe-Zeo-A (1.02 wt.%) and Fe-Silica (0.72 wt.%).



Supplementary Figure 2. TEM images of Fe-ZSM-5, Fe-Zeo-A, and Fe-Silica.

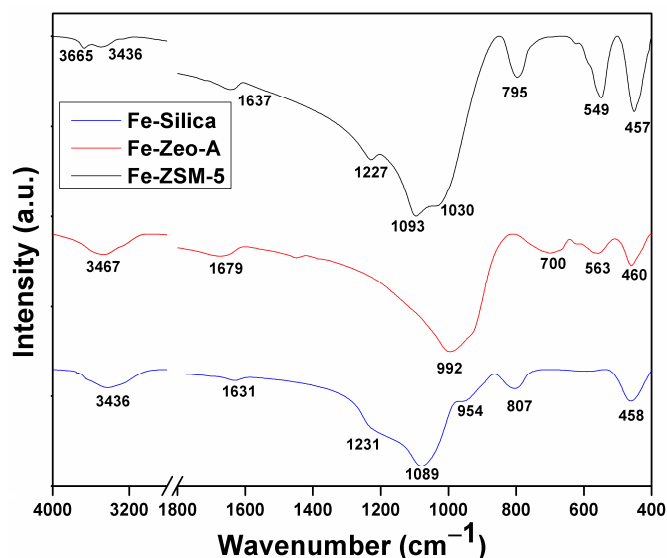
TGA: TGA analysis of Fe-ZSM-5, Fe-Zeo-A, and Fe-Silica have been represented in **Supplementary Figure 3**. For Fe-ZSM-5, Fe-Zeo-A, and Fe-Silica, 6.31%, 7.37%, and 5.74% of weight loss, respectively was recorded in the range of 30-200 °C. This could be assigned to the evaporation of free or physically adsorbed water molecules. The weight loss observed for Fe-ZSM-5 (0.98%), Fe-Zeo-A (0.97%), and Fe-Silica (0.31%) was due to the loss of water molecules from hydration spheres of Na and Fe ions. Slight variations were observed above 400 °C, probably due to dehydroxylation. This loss was prominent in Fe-Zeo-A due to the higher concentration of Na and Fe ions. Moreover, Fe-ZSM-5 was found more stable than Fe-Zeo-A due to a higher Si: Al ratio for Fe-ZSM-5 (~11.32) than Fe-Zeo-A (~1.34) as Si: Al ratio is directly proportional to the thermal stability of a zeolite. This direct proportionality is attributed to the variation of the lattice constant, which is related to Al–O (1.728 Å) and Si–O (1.608 Å) bond lengths. For Fe-Silica, another weight loss in the range of 700-1000 °C was due to a higher degree of dehydroxylation.



Supplementary Figure 3. TGA profiles of Fe-ZSM-5, Fe-Zeo-A, and Fe-Silica.

FTIR: In the FTIR spectra of catalysts (**Supplementary Figure 4**), the band in the range of 457-460 cm^{-1} has been assigned to the internal bending vibrations of SiO_4 tetrahedral units present in all the three adsorbents. The band at 549 cm^{-1} (Fe-ZSM-5) and 563 cm^{-1} (Fe-Zeo-A) have been assigned to the framework five-membered and four-membered structural units present in Fe-ZSM-5 and Fe-Zeo-A, respectively. The band at 795 cm^{-1} (Fe-ZSM-5), 700 cm^{-1} (Fe-Zeo-A), and 807 cm^{-1} (Fe-Silica) corresponded to the symmetric stretching vibrations of Si-O-T (T = Al for zeolites and Si for silica). The bands at 992 cm^{-1} (Fe-Zeo-A), 1030 cm^{-1} and 1093 cm^{-1} (Fe-ZSM-5), and 1089 cm^{-1} (Fe-Silica) corresponded to the asymmetric stretching vibrations of Si-O-T (T = Al for zeolites and Si for silica). The band at ~ 1631 -1679 cm^{-1} was due to the bending modes of the hydroxyl group of water molecules. The bands in the range of 3400-3700 cm^{-1} were assigned to stretching vibrations of T-OH and water molecules. The ratio of band intensities at 550 cm^{-1}

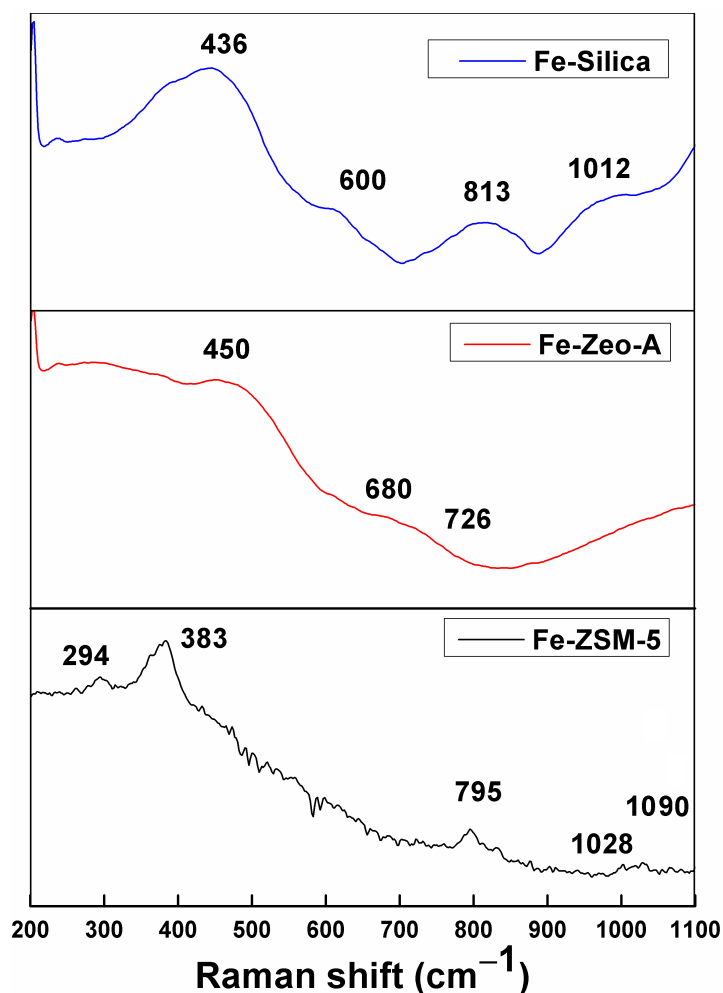
and 450 cm^{-1} is considered as a reliable index for evaluating the zeolite crystallinity. For Fe-ZSM-5, the $I_{552}/I_{458} \sim 0.817$ (> 0.8) index showed 100% crystallinity.



Supplementary Figure 4. FTIR spectra of Fe-ZSM-5, Fe-Zeo-A, and Fe-Silica.

Raman: The Raman spectrum of Fe-ZSM-5 showed bands at 294 cm^{-1} , 383 cm^{-1} , 795 cm^{-1} , 1028 cm^{-1} , and 1090 cm^{-1} (**Supplementary Figure 5**). The stronger band at 383 cm^{-1} was due to the ν_s (Si–O–Si) bending vibration of five-membered rings in the zeolitic framework. The peak at 294 cm^{-1} corresponded to the bending mode of six-membered rings. The sharp band at 795 cm^{-1} (symmetric) and bands at 1028 cm^{-1} and 1090 cm^{-1} (asymmetric) were assigned to the stretching vibration modes of Si–O/Al–O. For Fe-Zeo-A, the band at 450 cm^{-1} was the characteristic of four-membered framework rings. The bands at 680 cm^{-1} and 726 cm^{-1} were due to the vibrations of Al–O and Si–O bonds, respectively. In the Raman spectrum of Fe-Silica, the broad band centered at 436 cm^{-1} (ω_1) was assigned to the bending mode of oxygen in n -membered rings ($n > 4$) and the breathing mode of four-membered rings. The peak at 600 cm^{-1} is a characteristic three-membered ring breathing mode (D_2 line). The bands at 813 cm^{-1} (ω_3) and

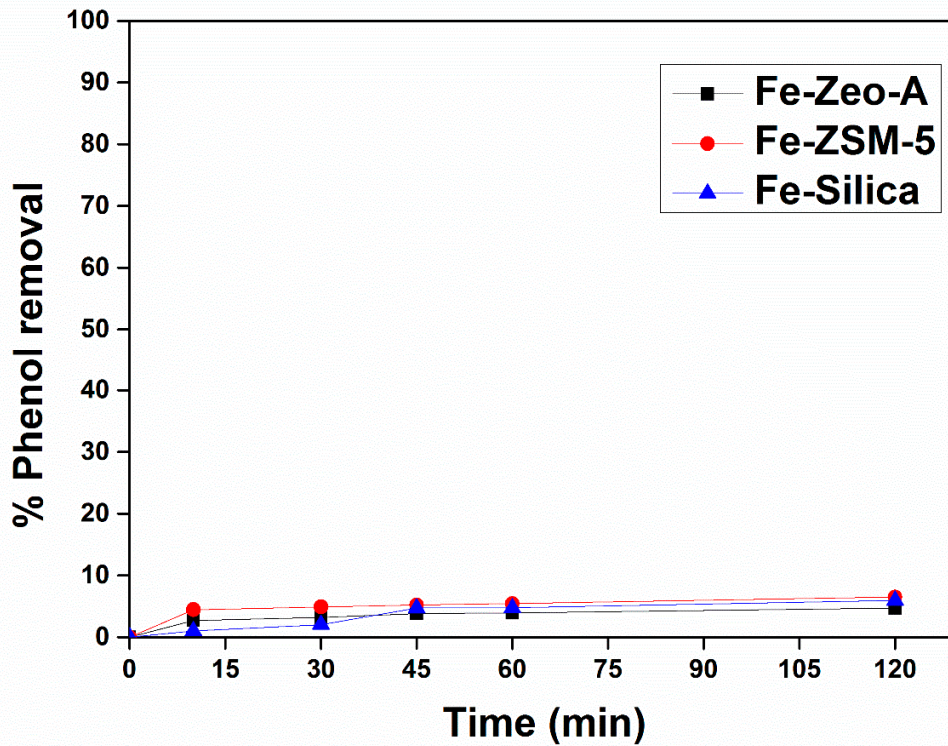
1012 cm^{-1} (ω_4) corresponded to the SiO_2 network optical mode and the Si–OH vibration mode with respect to Si, respectively [2].



Supplementary Figure 5. Raman spectra of Fe-ZSM-5, Fe-Zeo-A, and Fe-Silica

Supplementary Table 3. Lattice parameters of Fe-ZSM-5.

Catalysts	a (Å)	b (Å)	c (Å)	V (Å ³)
Fe-ZSM-5	21.534	20.106	13.690	5927.255
Fe-ZSM-5-H ₂ O ₂	21.676	20.179	13.789	6031.333



Supplementary Figure 6. Adsorption of phenol onto Fe-ZSM-5, Fe-Zeo-A, and Fe-Silica

Supplementary Table 4. Elemental analysis of Fe-ZSM-5, Fe-Zeo-A, and Fe-Silica after phenol degradation *via* photo-Fenton process.

Element	Fe-ZSM-5	Fe-Zeo-A	Fe-Silica
	Weight%	Weight%	Weight%
O	64.35	63.56	65.83
Na	0.46	2.51	-
Al	2.88	13.78	-

Si	31.06	19.23	33.81
Fe	1.25	0.92	0.36

References

1. M. Thommes, K. Kaneko, A. V. Neimark, J. P. Olivier, F. Rodriguez-Reinoso, J. Rouquerol, K. S. W. Sing, *Pure Appl. Chem.* 87 (2015) 1051-1069.
2. L. Spallino, L. Vaccaro, L. Sciortino, S. Agnello, G. Buscarino, M. Cannas, F. M. Gelardia, *Phys. Chem. Chem. Phys.* 16 (2014) 22028-22034.